Mechanical Technology and Engineering Insights

www.mtei-reapress.com

Mech. Technol. Eng. Insights. Vol. 3, No. 1 (2026) 16–28.

Paper Type: Original Article

Free Convection Heat Transfer with Thermal Radiation over Vertical Wavy Surfaces

Lorenzo Cevallos-Torres[1,*], Motahare Mahmoodnezhad[2]

[1] Brigham Young University–Idaho, USA; cev18002@byui.edu.

[2] Department of Mechanical Engineering, Shahrood University of Technology, Shahrood, Semnan, Iran; motahare.mahmoodnezhad@gmail.com.

Citation:

Received: 12 August 2025 *Revised: 22 October 2025* *Accepted: 24 December 2026*	Cevallos-Torres, L., & Mahmoodnezhad, M. (2026). Free convection heat transfer with thermal radiation over vertical wavy surfaces. *Mechanical Technology and Engineering Insights, 3*(1), 16-28.

Abstract

In this study, free convective boundary-layer heat transfer with the influence of thermal radiation over a vertical wavy surface is numerically investigated. A suitable coordinate transformation is applied to map the governing equations of the wavy surface onto an equivalent flat surface, thereby simplifying the mathematical formulation. The transformed, coupled nonlinear partial differential equations are solved using an efficient cubic spline numerical method. The effects of key dimensionless parameters, including the radiation parameter, surface heating parameter, Prandtl number, and wave amplitude, on the flow and thermal characteristics are systematically examined. Variations in the local and average Nusselt numbers as well as the skin friction coefficient are presented and discussed in detail. The numerical results reveal that increasing the radiation parameter significantly enhances the overall heat transfer rate. Moreover, it is observed that higher surface heating intensifies both velocity and temperature fields within the boundary layer, leading to an increase in the local and average Nusselt numbers. The findings provide useful physical insight into the combined effects of surface waviness and thermal radiation on natural convection heat transfer, which can be beneficial in the design of thermal systems involving complex surface geometries.

Keywords: Free convection heat transfer, Thermal radiation, Vertical wavy surfaces, Cubic spline numerical method.

1 | Introduction

In recent years, the application of wavy surfaces has gained considerable practical importance due to the surface irregularities commonly encountered in industrial processes. Such surfaces are widely used in thermal engineering applications, including heat-dissipating fins, solar collectors, condensers, and related systems. Another important application of wavy surfaces is their utilization in the design and fabrication of plate heat exchangers, where surface waviness can significantly enhance heat transfer performance.

Corresponding Author: cev18002@byui.edu

https://doi.org/10.48313/mtei.v3i1.76

Licensee System Analytics. This article is an open-access article distributed under the terms and conditions of the Creative Commons Attribution (CC BY) license (http://creativecommons.org/licenses/by/4.0).

Several studies have been conducted on heat transfer over wavy surfaces. Hady et al. [1] investigated free convective heat transfer over a wavy surface in a porous medium in the presence of a magnetic field, considering the effects of internal heat generation or absorption. They solved the transformed nonlinear boundary-layer equations using the Runge–Kutta integration method combined with the shooting technique. The influence of wave amplitude along the surface on velocity and temperature profiles at a specific location was examined. Their results showed that increasing the velocity enhanced both heat generation and absorption effects. At the same time, the temperature profile decreased in the case of heat absorption and increased in the presence of heat generation.

Furthermore, their analysis of Magnetohydrodynamic (MHS) effects indicated that an increase in magnetic field strength led to higher temperature levels and reduced velocity. They also demonstrated that decreasing the heat generation/absorption parameter QQQ resulted in a reduction of both velocity and temperature at a given streamwise location along the surface.

In another study, Mamun and Hossain [2] examined heat transfer characteristics over wavy surfaces considering the influence of thermal radiation. Their work highlighted the significant role of radiative effects on the thermal behavior of natural convection flows over complex geometries. They analyzed the effect of thermal radiation on wavy surfaces using two numerical approaches, namely the finite difference method and the Keller–Box scheme. Their numerical results were illustrated through streamlines and isotherms. They reported that increasing both the surface temperature and the fluid temperature leads to an enhancement of the local Nusselt number and, consequently, the average Nusselt number. In addition, the influence of the radiation parameter (Planck number) on the velocity and temperature profiles was examined, and it was shown that higher values of this parameter result in increased fluid velocity and temperature. The results further indicated that the increase in temperature gradients associated with higher radiation parameters leads to an increase in the Nusselt number as well as the average heat transfer coefficient.

Other notable investigations on heat transfer over wavy surfaces include the study of heat transfer over composite wavy surfaces by Tashtoush and Al-Odat [3], natural convection heat transfer of Newtonian fluids by Kim [4], mixed convection heat transfer with magnetohydrodynamic effects by Chang and Chen [5], mixed convection of micropolar fluids by Chang and Chen [6], and natural heat and mass transfer by Chang, Liu, and co-workers [7]. Convection heat transfer is one of the three fundamental modes of heat transfer, the other two being conduction and radiation. In most practical engineering applications, at least two modes of heat transfer occur simultaneously.

Accordingly, the present study focuses on free convective heat transfer of a fluid with the inclusion of thermal radiation over a vertical wavy surface, where the surface temperature is higher than the ambient temperature. A simple coordinate transformation is employed to map the wavy surface onto a flat surface, after which the transformed boundary-layer equations are solved using the cubic spline numerical method. The effects of key parameters, including thermal radiation, surface heating, wave amplitude, and the Prandtl number, are investigated in terms of the local Nusselt number, average Nusselt number, and skin friction coefficient.

Rahman and Ahmad [8] numerically investigate the dynamics of shear-thinning non-Newtonian nanofluids containing living microorganisms over a gravitationally affected wavy surface under the influence of thermal radiation. By employing a modified approximation scheme, the research analyzes how key parameters like Richardson number and radiation factors enhance heat transfer and bioconvection performance in these complex materials [8]. Sarthak, In their paper, this study provides an in-depth analysis of the combined effects of surface waves, fluid inertia, and thermal radiation on natural convection within a porous medium under the influence of MHD bioconvection. By leveraging Physics-Informed Neural Networks (PINNs), this research examines the impact of various physical parameters and deep learning architectures on heat, mass, and microorganism density transfer [9–11].

Ullah [12], In their paper, the authors perform a numerical investigation into magnetic fluid flow along a vertical surface, focusing on the effects of variable viscosity and porous media on thermal management. Utilizing the Keller-box method, the research demonstrates how reduced gravity and porosity influence fluid

velocity, heat transport, and magnetic flux in industrial heat exchanger applications [8]. Ashfag [13], the authors examine the boundary layer flow over a moving horizontal surface in a nanofluid, accounting for viscous dissipation, flexible heating, and the presence of gyrotactic microorganisms. Utilizing the bvp4c solver in MATLAB, the study systematically evaluates the impact of temperature-dependent thermal conductivity and magnetic fields on enhancing heat transfer efficiency and the thermophysical properties of base fluids.

2 | Mathematical Formulation

The boundary-layer flow of the fluid under consideration passes over a semi-infinite body with a vertical wavy surface. The vertical wavy surface is described by

$$\sigma(\bar{x}) = \bar{a}\sin\left(n\pi x / L\right), \tag{1}$$

where $\bar{a}$ denotes the wave amplitude and L represents the wavelength. The wavy surface of the body is maintained at a constant temperature, T_w which is higher than the ambient temperature T_∞. The free-stream velocity as well as the inlet velocity at the leading edge of the plate are both zero. *Fig. 1* illustrates the physical model and the corresponding coordinate system .The problem geometry is illustrated in the figure. In this coordinate system, x is defined along the wavy plates in the flow direction, and y is perpendicular to the flow. Furthermore, the fluid flow is assumed to be laminar, incompressible, steady, and two-dimensional. The effects of viscous dissipation are neglected. Consequently, considering the influence of thermal radiation, the governing equations are formulated as follows.

$$\frac{\partial \bar{u}}{\partial \bar{x}} + \frac{\partial \bar{v}}{\partial \bar{y}} = 0. \tag{2}$$

$$\rho\left(\bar{u}\frac{\partial \bar{u}}{\partial \bar{x}} + \bar{v}\frac{\partial \bar{u}}{\partial \bar{y}}\right) = -\frac{\partial \bar{p}}{\partial \bar{x}} + \left(\frac{\partial \tau_{\bar{x}\bar{x}}}{\partial \bar{x}} + \frac{\partial \tau_{\bar{x}\bar{y}}}{\partial \bar{y}}\right) + \rho g\beta\left(T - T_\infty\right). \tag{3}$$

$$\rho\left(\bar{u}\frac{\partial \bar{v}}{\partial \bar{x}} + \bar{v}\frac{\partial \bar{v}}{\partial \bar{y}}\right) = -\frac{\partial \bar{p}}{\partial \bar{y}} + \left(\frac{\partial \tau_{\bar{y}\bar{x}}}{\partial x} + \frac{\partial \tau_{\bar{y}\bar{y}}}{\partial \bar{y}}\right). \tag{4}$$

$$\rho C_p\left(\bar{u}\frac{\partial T}{\partial \bar{x}} + \bar{v}\frac{\partial T}{\partial \bar{y}}\right) = K_f\left(\frac{\partial^2 T}{\partial \bar{x}^2} + \frac{\partial^2 T}{\partial \bar{y}^2}\right) - \nabla q_r. \tag{5}$$

The corresponding boundary conditions for this system are given by

I. On the wavy boundary $T = T_w, \bar{u} = \bar{v} = 0.$

II. At the free surface $\bar{y} \to \infty,\ T \to T_\infty, \bar{u} = 0.$

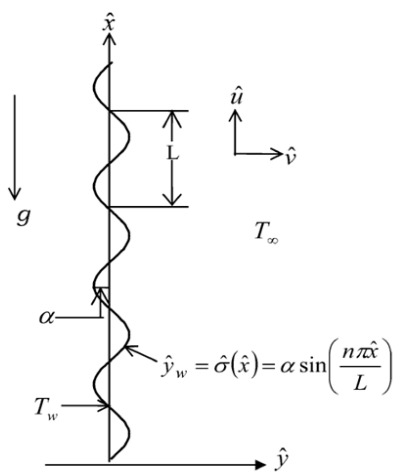

Fig. 1. Physical model and coordinate system of the problem.

In the above equations, $\bar{u}$, $\bar{v}$, denote the components of the fluid velocity vector in the $\bar{x}$, $\bar{y}$, directions, respectively; ρ is the fluid density; $\bar{p}$ is the pressure; C_p, epresents the specific heat capacity of the fluid at constant pressure; q_r is the radiative heat flux; and T, β denote the fluid temperature and the thermal expansion coefficient, respectively. The radiative heat flux, q_r, in the y-direction is expressed using the Rosseland diffusion approximation as follows:

$$q_r = -\frac{4\sigma^*}{3k(\alpha_r + \sigma_s)}\nabla T^4,$$

where σ^* α_r, σ_s denote, respectively, the Stefan–Boltzmann constant, the Rosseland mean absorption coefficient, and the scattering coefficient. The limitations of the diffusion approximation must also be taken into account. This expression is valid in the interior regions, sufficiently far from the boundaries; however, it is not applicable in the vicinity of boundaries. Consequently, it is suitable for strongly absorbing media with a thick boundary-layer film. Therefore, it does not provide a complete description of the physical situation, since it does not include any radiation term at the boundary surface.

Using the Prandtl transformation to map the wavy surface onto a flat surface, as proposed by Yao [14], the dimensionless variables employed for nondimensionalizing the governing equations are defined as follows:

$$\begin{aligned} &x^* = \frac{x}{L}, y^* = \frac{y-\bar{\sigma}}{L}Gr^{1/4}, u^* = \frac{\rho L}{\mu Gr^{1/2}}u,. \\ &v^* = \frac{\rho L}{\mu Gr^{1/2}}(v - \sigma' u), Gr = \frac{g\beta(T_w - T_\infty)\rho^2 L^3}{\mu^2}. \\ &Pr = \frac{\mu C_p}{K}, \theta = \frac{T - T_\infty}{T_w - T_\infty}, P^* = \frac{\rho L^2}{\mu^2 Gr}P, \sigma = \frac{\bar{\sigma}}{L}. \end{aligned} \tag{6}$$

By substituting the dimensionless variables given in *Eq. (6)* into *Eqs. (1)–(5)*, we obtain:

$$\frac{\partial u^*}{\partial x^*} + \frac{\partial v^*}{\partial y^*} = 0.$$

$$u^*\frac{\partial u^*}{\partial x^*} + v^*\frac{\partial u^*}{\partial y^*} = -\frac{\partial p^*}{\partial x^*} + \sigma'\frac{\partial p^*}{\partial y^*}Gr^{1/4} + (1+\sigma'^2)\frac{\partial^2 u^*}{\partial y^{*2}} + \theta.$$

$$u^{*2}\sigma'' + \sigma'(\theta) = \sigma'\frac{\partial p^*}{\partial x^*} - (1+\sigma'^2)\frac{\partial p^*}{\partial y^*}Gr^{1/4}.$$

$$u^*\frac{\partial \theta}{\partial x^*} + v^*\frac{\partial \theta}{\partial y^*} = \frac{1}{Pr}(1+\sigma'^2)\frac{\partial}{\partial y^*}\left[\left\{1 + \frac{4}{3}R_d\left(1 + (\theta_w - 1)\theta\right)^3\right\}\frac{\partial \theta}{\partial y^*}\right]\theta,$$

where, in the above relation, the radiative conduction term (Planck number) and the surface heat term are defined as follows:

$$R_d = \frac{4\sigma^* T_\infty^{\,3}}{K(\alpha_r + \sigma_s)}, \theta_w = \frac{T_w}{T_\infty}\mathbb{S}. \tag{7}$$

As can be observed from *Eq. (9)*, the pressure gradient in the y -direction is nonzero $O(Gr^{-1/4})$, whereas the pressure gradient in the x-direction is obtained by solving the inviscid flow. In the present study, by neglecting the pressure gradient in the x -direction and $\partial p^* / \partial y^*$ eliminating the pressure term using *Eqs. (9)* and *(10)*, the momentum equation can be reduced to a single equation. Therefore, we have:

$$u^*\frac{\partial u^*}{\partial x^*} + v^*\frac{\partial u^*}{\partial y^*} = \frac{1}{(1+\sigma'^2)}(\theta - u^{*2}\sigma'\sigma'') + (1+\sigma'^2)\frac{\partial^2 u^*}{\partial y^{*2}}. \tag{8}$$

Since point $x = 0$ is a singular point, the following transformations are employed in order to remove this singularity:

$$X = x^*; Y = \frac{y^*}{(4x^*)^{1/4}}; U = \frac{u^*}{(4x^*)^{1/2}}; V = (4x^*)^{1/4} v^*.$$

By substituting *Eq. (13)* into *Eqs. (7), (10),* and *(12)*, the final governing equations are obtained in the following form:

$$2U + 4X\frac{\partial U}{\partial X} - Y\frac{\partial U}{\partial Y} + \frac{\partial V}{\partial Y} = 0. \tag{9}$$

$$4XU\frac{\partial U}{\partial X} + (V - UV)\frac{\partial U}{\partial Y} + (2 + \frac{4X\sigma'\sigma''}{1+\sigma'^2})U^2 + \frac{1}{1+\sigma'^2}(\theta) + (1+\sigma'^2)\frac{\partial^2 U}{\partial Y^2}. \tag{10}$$

$$4XU\frac{\partial \theta}{\partial X} + (V - UY)\frac{\partial \theta}{\partial Y} = \frac{1}{Pr}(1+\sigma'^2)\frac{\partial}{\partial Y}\left[\left\{1 + \frac{4}{3}R_d\left(1 + \left(\theta_w - 1\right)\theta\right)^3\right\}\frac{\partial \theta}{\partial Y}\right]. \tag{11}$$

Subject to the following boundary conditions:

$$Nu_{\bar{x}} = \frac{\bar{x}\left[-\left(k\bar{n}.\nabla T\right) + \bar{n}.q_r\right]}{K_f\left(T - T_\infty\right)}. \tag{12}$$

Accordingly, using Newton's law of cooling and after applying the transformations, the following expressions for the local Nusselt number can be written as

$$Nu_{\bar{x}} = -\left(\frac{Gr}{4x}\right)^{1/4}\left(1 + S'^2\right)^{1/2}\left(1 + \frac{4}{3}R_d\theta_w{}^3\right)\left.\frac{\partial \theta}{\partial y}\right|_{y=0}. \tag{13}$$

Furthermore, the average Nusselt number is obtained using the following formula:

$$Nu_m Gr^{-1/4} = -\frac{1}{S}\int_0^x \left(\frac{1}{4x}\right)^{1/4}\left(1 + S'^2\right)\left(1 + \frac{4}{3}R_d\theta_w{}^3\right)\left.\frac{\partial \theta}{\partial y}\right|_{y=0} dx, \tag{14}$$

where

$$S = \int_0^x \left(1 + S'^2\right)^{1/2} dx. \tag{15}$$

The friction coefficient is defined as follows:

$$C_f = \frac{2\tau_w}{\rho \tilde{U}^2}, \tag{16}$$

where,

$$\tilde{U} = \frac{\mu Gr^{1/2}}{\rho L}, \tag{17}$$

which represents the characteristic velocity. Therefore, the dimensionless form of the friction coefficient is expressed as follows.

$$C_f = \left(\frac{4x}{Gr}\right)^{1/4} 2\left(1 + S'^2\right)\left(\frac{\partial u}{\partial y}\right)_{y=0}. \tag{18}$$

2.1 | Numerical Solution Method

The system of differential *equations (14)–(16)* is solved numerically using the Spline Alternating Direction Implicit (SADI) method [9], [15], subject to the prescribed boundary conditions. In the numerical procedure, the governing equations are initially treated as unsteady, and the time-marching process is continued until a steady-state solution is achieved. Furthermore, *Eqs. (15)* and *(16)* may be rewritten in the following generalized form:

$$\varphi_{i,j} = F_{i,j}^{n} + G_{i,j} m_{i,j}^{n+1} + S_{i,j} M_{i,j}^{n+1}, \tag{19}$$

where Iand denote the computational nodes, and n represents the time step φ, u θ. Substituting the first and second derivatives of φ (or your specific variable) with respect to y, denoted by m and M, respectively, into the governing equations. Furthermore, by employing the order reduction method [9], *Eq. (24)* can be reformulated as follows:

$$\varphi_{i,j} = F_{i,j}^{n} + G_{i,j} m_{i,j}^{n+1} + S_{i,j} M_{i,j}^{n+1}, \tag{20}$$

Thus, the corresponding terms Ω are replaced by their first- and second-order derivatives u. It should be θ noted that *Eq. (25)* has a tridiagonal structure and can therefore be efficiently solved using the Thomas algorithm. The solution procedure is continued until the desired convergence criterion is satisfied. The convergence criterion is defined as follows.

$$\frac{\Omega_{i,j}^{n+1} - \Omega_{i,j}^{n}}{\Omega_{max}^{n}} < 5 \times 10^{-5}. \tag{21}$$

5 | Discussion

Since the cubic spline method does not require the use of a symmetric grid, and considering that the gradients of temperature and velocity exhibit larger variations near the wavy wall in the y direction as well as near the leading edge of the plate in the x direction, a finer grid is employed in the aforementioned regions. Figure 2 illustrates the grid distribution used in the present study.

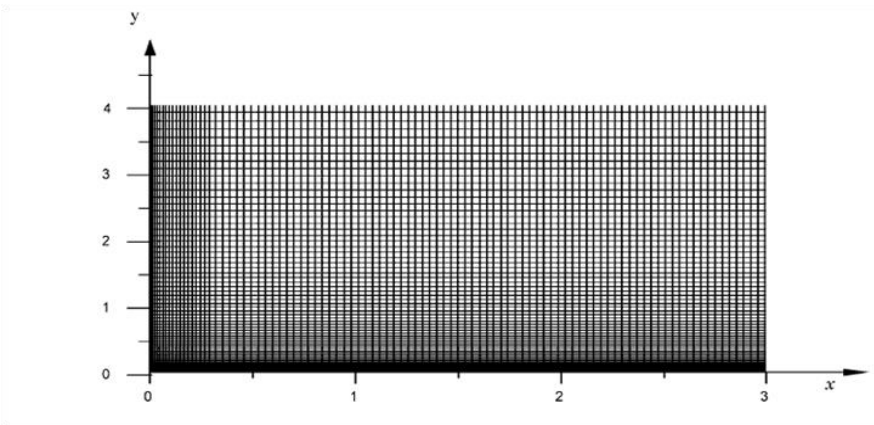

Fig. 2. Computational grid distribution.

One of the most important issues in numerical simulations is ensuring that the number of grid points is sufficient. In order to achieve an appropriate and adequate number of grid points, the computations are initially started with a suitable grid, and then the number of grid points is gradually increased such that, beyond a certain grid size, the effect of the mesh on the results becomes negligible. For the present problem, grid sizes of 250×100250, 300×150300, 400×200400, and 500×250500 are employed. The corresponding results,

in terms of the Nusselt number and skin friction coefficient at various locations, are presented in *Table 1*. The results indicate that the difference between the 400×200400and 500×250500 grids is less than 1% for $R_d = \theta_w = Q = 0.0$, $Pr = 10$, $\alpha = 0.0$. Furthermore, the present results are compared with those reported by Chiu and Chou [11] and Kumari et al. [16] in *Table 2*.

Table 1. Heat transfer coefficient and skin friction coefficient for different grid resolutions $Pr = 1.0, \alpha = 0, R_d = \theta_w = Q = 0$.

Grid size	$Nu_{\bar{x}}\left(\frac{4X}{Gr}\right)^{1/4}$ at		$C_f\left(\frac{4X}{Gr}\right)^{1/4}$ at	
	(x=0.1)	(x=0.4)	(x=0.1)	(x=0.4)
100 × 250	1.19856	1.18198	0.53091	0.53708
150 × 300	1.19502	1.17941	0.53430	0.53725
200 × 400	1.19625	1.18106	0.53350	0.53658
250 × 500	1.19743	1.18395	0.53387	0.53436

Table 2. Comparison of the local Nusselt number $Nu_x(4X/Gr)^{1/4}$ $\alpha = 0.1, Pr = 1.$, $R_d = \theta_w = Q = 0$.

(X)	Present	Kumari et al. [16]	Chiu and Chou [11]
1.5	0.533551	0.53634	0.535919
1.75	0.545391	0.54810	0.562036
2.0	0.533588	0.53709	0.534797
2.25	0.544652	0.54732	0.562414
2.5	0.533216	0.53762	0.533628

Figs. 3 and *4* illustrate the variations of the local Nusselt number $Nu_x(4X/Gr)^{1/4}$ and average Nusselt number $(Nu_m / Gr^{1/4})$ $Pr = 0.7, \theta_w = 1.1, \alpha = 0.2$ for various radiation parameters. The results indicate that an increase in the radiation parameter leads to an enhancement in both local and average Nusselt numbers. This can be attributed to the intensified interaction of radiation within the thermal and hydraulic boundary layers as R_d increases; consequently, the fluid's heat absorption capacity is augmented, leading to an increase in flow velocity. *Figs. 5* and *6* present the temperature and velocity profiles for different values of R_d. It is observed that higher radiation values result in elevated temperature and velocity magnitudes. Furthermore, both thermal and momentum boundary layer thicknesses exhibit a slight increase. This phenomenon occurs because an increase in R_d enhances the velocity gradient, thereby accelerating the fluid flow. Accordingly, the velocity distribution is further promoted due to the enhanced heat absorption intensity of the fluid.

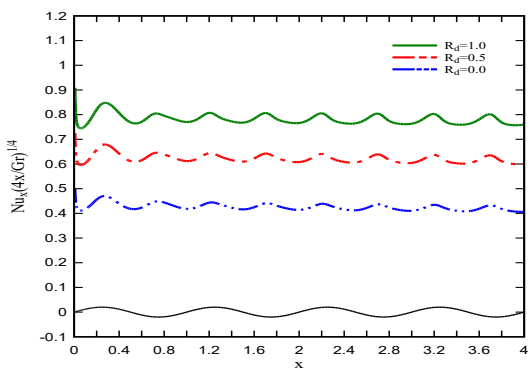

Fig. 3. Variation of the local Nusselt number $Nu_x(4X/Gr)^{1/4}$ at $Pr = 0.7, \theta_w = 1.1, \alpha = 0.2$ various values of R_d.

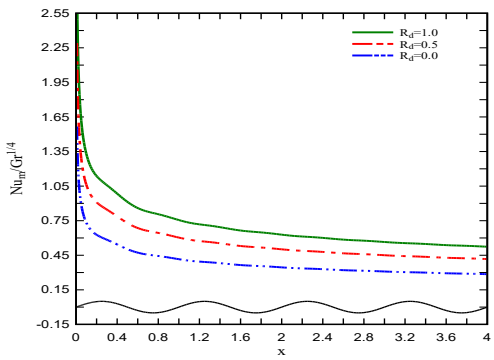

Fig. 4. Variation of the average Nusselt number $\left(Nu_m / Gr^{1/4}\right)$ for $Pr = 0.7, \theta_w = 1.1, \alpha = 0.2$ various values of R_d.

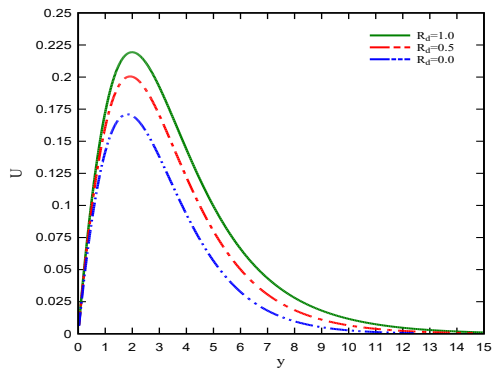

Fig. 5. Temperature profiles $Pr = 0.7, \theta_w = 1.1, \alpha = 0.2$, and various values of R_d at x=1.0.

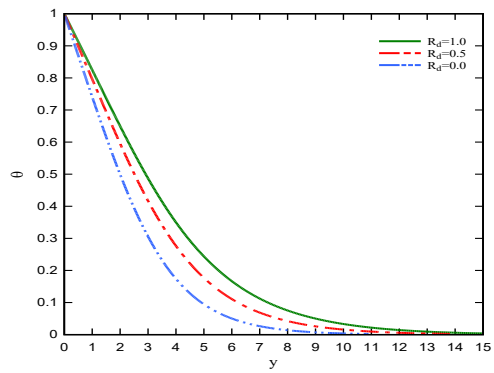

Fig. 6. Velocity profiles $Pr = 0.7, \theta_w = 1.1, \alpha = 0.2$, and various values of R_d at x=1.0.

The heat transfer behavior is shown in *Figs. 7* and *8* for various values of the surface heat parameter and the local and average Nusselt numbers $Pr = 1.0, R_d = 1.0, \alpha = 0.15$.. It is evident that when the surface heat parameter increases, both the average and local Nusselt numbers rise.

The main cause of this improvement is the increase in surface temperature brought on by increased surface heat values, which exacerbates the temperature differential between the heated surface and the surrounding fluid. Higher local and average Nusselt numbers come from this strengthening of the convective heat transfer rate.

Additionally, the temperature and velocity profiles corresponding to different surface heat parameter values are shown in *Figs. 9* and *10*. The findings show that both the fluid temperature and velocity fields are greatly increased by an increase in the surface heat parameter.

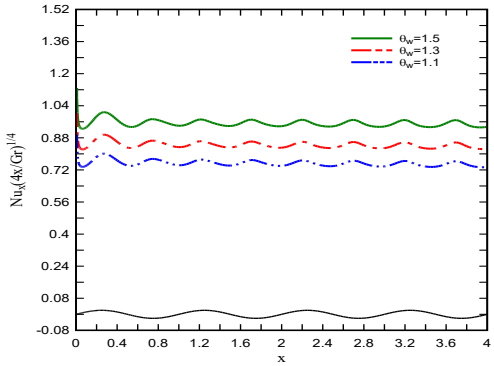

Fig. 7. Variation of the local Nusselt number $Nu_x(4X/Gr)^{1/4}$ at $Pr = 1.0, R_d = 1.0, \alpha = 0.15$ various values of θ_w.

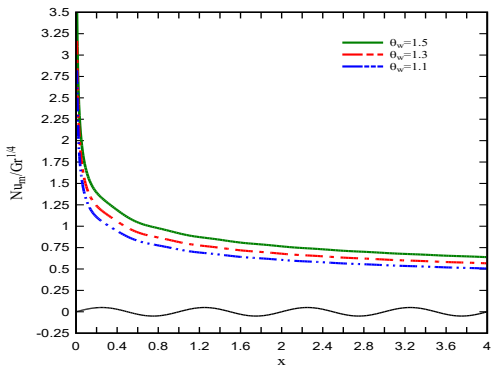

Fig. 8. Variation of the average Nusselt number $\left(Nu_m/Gr^{\frac{1}{4}}\right)$ at $Pr = 1.0,\ R_d = 1.0, \alpha = 0.15$, and various values of θ_w.

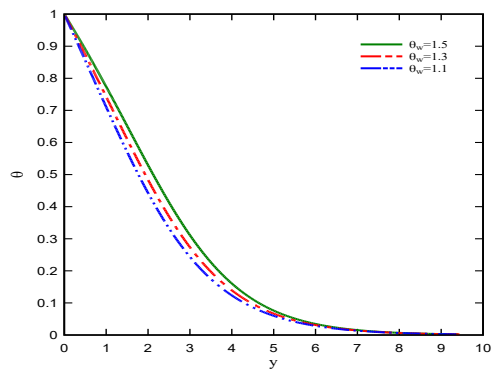

Fig. 9. Temperature profiles for $Pr = 1.0,\ R_d = 1.0, \alpha = 0.15$, and various values of θ_w x=1.0.

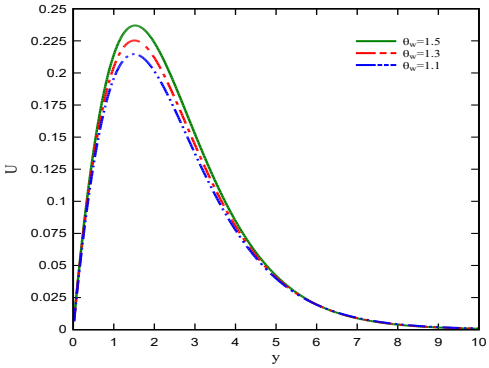

Fig. 10. Velocity profile for $Pr = 1.0, R_d = 1.0, \alpha = 0.15$ various values of θ_w and x=1.0.

Figs. 11-13 illustrate the variations of the local Nusselt number, average Nusselt number, and skin friction coefficient for $\theta_w = 1.3, R_d = 1.0, \alpha = 0.25$ different Prandtl numbers. The results indicate that the skin friction coefficient decreases as the Prandtl number increases. This behavior can be attributed to the fact that lower density enhances the sensitivity to buoyancy effects, which leads to more significant variations in the wall velocity gradient (see *Fig. 15*), thereby increasing the skin friction coefficient. On the other hand, an increase in the Prandtl number enhances the temperature gradient (see *Fig. 14*), resulting in higher local and average Nusselt numbers. Furthermore, as shown in *Figs. 14* and *15*, both the thermal and velocity boundary layer thicknesses decrease with an increase in the Prandtl number.

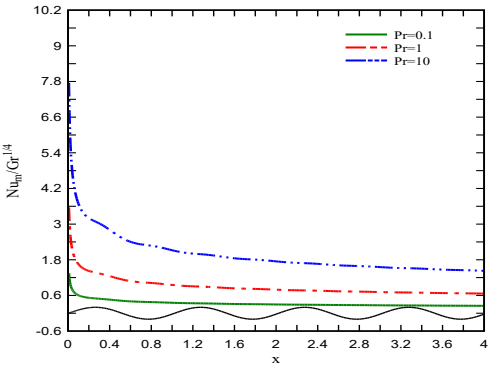

Fig. 12. Variation of the average Nusselt number $\left(Nu_m / Gr^{1/4}\right)$, $\theta_w = 1.3, R_d = 1.0, \alpha = 0.25$ for different Prandtl numbers.

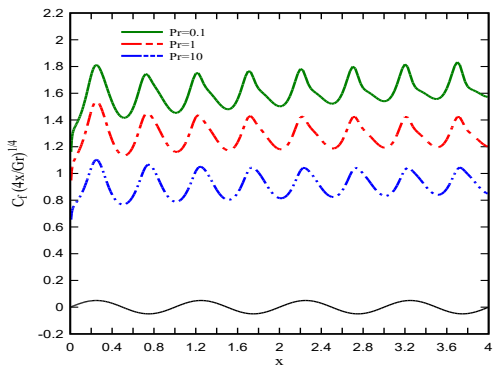

Fig. 13. Variation of the skin friction coefficient for $C_f\left(4X/Gr\right)^{1/4}$ $\theta_w = 1.3, R_d = 1.0, \alpha = 0.25$ different Prandtl numbers.

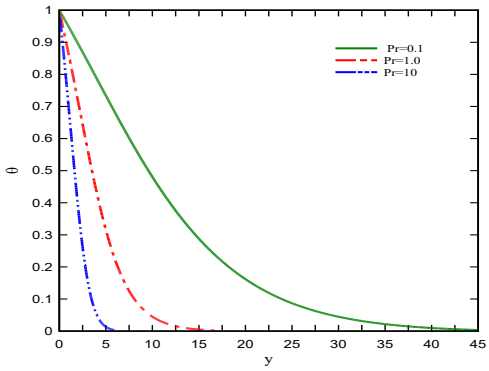

Fig. 14. Temperature profiles for $\theta_w = 1.3, R_d = 1.0, \alpha = 0.25$ different Prandtl numbers at x=1.0.

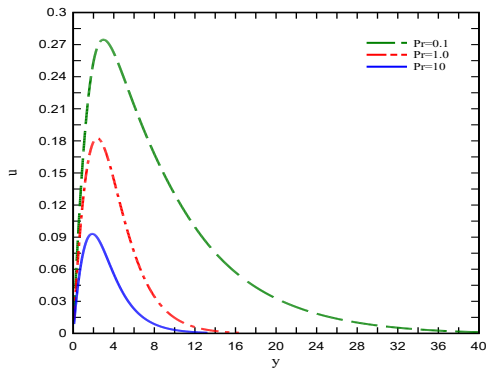

Fig. 15. Velocity profiles for $\theta_w = 1.3, R_d = 1.0, \alpha = 0.25$ different Prandtl numbers at x=1.0.

The fluctuations of the local Nusselt number, average Nusselt number, and skin friction coefficient for $\theta_w = 1.2, R_d = 1.0, Pr = 1.0,$ various wave amplitude values (α = 0.05, 0.10,0.20). The findings unequivocally show that raising the wave amplitude considerably lowers the skin friction coefficient as well as the local and average Nusselt values. Larger wave amplitudes physically exacerbate surface undulations, creating recirculation zones and flow separation close to the wavy wall. These events lower the temperature gradient at the wall and reduce the wall shear stress by thickening the thermal and hydrodynamic boundary layers. As a result, there is less convective heat transfer, which lowers Nusselt.

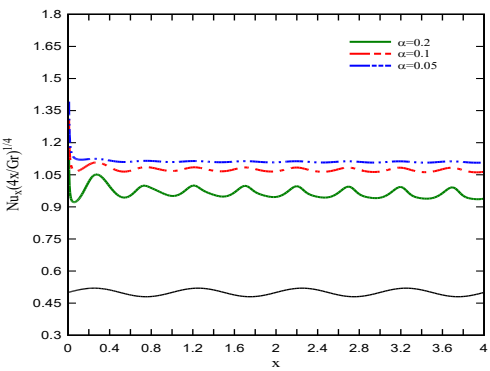

Fig. 16. Variation of the local Nusselt number $Nu_x(4X/Gr)^{1/4}$ for $\theta_w = 1.2, R_d = 1.0, Pr = 1.0$ various wave amplitude values.

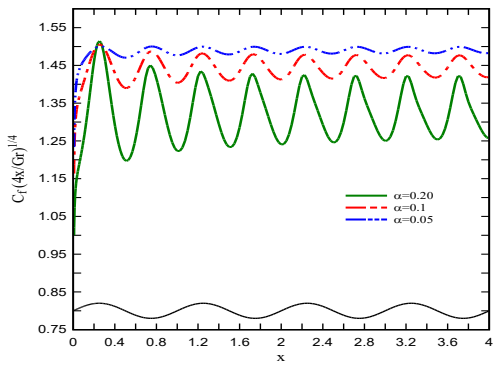

Fig. 17. Variation of the skin friction coefficient for $C_f(4X/Gr)^{1/4}$ $\theta_w = 1.2, R_d = 1.0, Pr = 1.0$ various wave amplitude values.

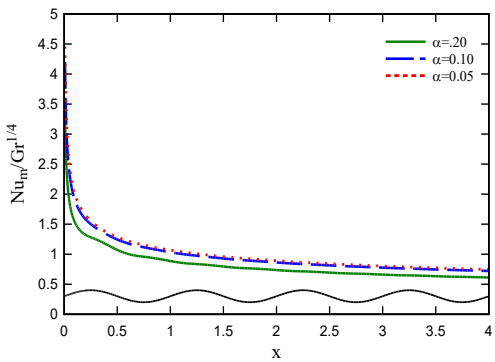

Fig. 18. Variation of the average Nusselt number for $(Nu_m / Gr^{1/4})$ $\theta_w = 1.2, R_d = 1.0, Pr = 1.0$ various wave amplitude values.

5 | Conclusion

Free convection heat transfer across a vertical wavy surface with thermal radiation effects was examined numerically in this work. A Prandtl-type transformation was used to translate the wavy geometry onto a flat surface, and the cubic spline SADI approach was used to solve the governing equations. The findings show that by speeding the fluid and enhancing convective heat transport, raising the radiation parameter raises both local and average Nusselt numbers. Improved heat transfer rates result from higher surface heat, which also raises the temperature and velocity fields. By steepening the temperature gradient, raising the Prandtl number improves Nusselt numbers while marginally lowering skin friction.

On the other hand, because of flow separation and thicker boundary layers close to the wavy wall, bigger wave amplitudes decrease heat transmission and skin friction. These results offer useful advice. These results offer useful recommendations for the design of thermal systems with intricate surface geometries where natural convection and radiation play a major role.

Conflict of Interest

The authors declare that there is no conflict of interest regarding the publication of this article.

Data Availability

All data generated or analyzed during this study are included in this published article. No additional data are available.

Funding

This research did not receive any specific grant from funding agencies in the public, commercial, or not-for-profit sectors.

Reference

[1] Hady, F. M., Mohamed, R. A., & Mahdy, A. (2006). MHD free convection flow along a vertical wavy surface with heat generation or absorption effect. *International communications in heat and mass transfer*, *33*(10), 1253–1263. https://doi.org/10.1016/j.icheatmasstransfer.2006.06.007

[2] Molla, M. M., & Hossain, M. A. (2007). Radiation effect on mixed convection laminar flow along a vertical wavy surface. *International journal of thermal sciences*, *46*(9), 926–935. https://doi.org/10.1016/j.ijthermalsci.2006.10.010

[3] Tashtoush, B., & Al-Odat, M. (2004). Magnetic field effect on heat and fluid flow over a wavy surface with a variable heat flux. *Journal of magnetism and magnetic materials*, *268*, 357–363. https://doi.org/10.1016/S0304-8853(03)00547-X

[4] Kim, E. (1997). Natural convection along a wavy vertical plate to non-Newtonian fluids. *International journal of heat and mass transfer*, *40*(13), 3069–3078. https://doi.org/10.1016/S0017-9310(96)00357-2

[5] Wang, C. C. (2005). Mixed convection boundary layer flow on inclined wavy plates including the magnetic field effect. *International journal of thermal sciences*, *44*(6), 577–586. https://doi.org/10.1016/j.ijthermalsci.2005.02.001

[6] Wang, C. C., & Chen, C. K. (2001). Transient force and free convection along a vertical wavy surface in micropolar fluids. *International journal of heat and mass transfer*, *44*(17), 3241–3251. https://doi.org/10.1016/S0017-9310(00)00329-X

[7] Jang, J. H., Yan, W. M., & Liu, H. C. (2003). Natural convection heat and mass transfer along a vertical wavy surface. *International journal of heat and mass transfer*, *46*(6), 1075–1083. https://doi.org/10.1016/S0017-9310(02)00361-7

[8] Rahman, A. U., & Ahmad, L. (2025). Mixed convective and radiative wavy motion of Williamson fluid in the presence of microorganisms. *Journal of radiation research and applied sciences*, *18*(1), 101271. https://doi.org/10.1016/j.jrras.2024.101271

[9] Wang, P., & Kahawita, R. (1983). Numerical integration of partial differential equations using cubic splines. *International journal of computer mathematics*, *13*(3–4), 271–286. https://doi.org/10.1080/00207168308803369

[10] Taha, M. S., Ates, A., Canli, E., & Altun, A. H. (2025). Circular perforations on vertically sinusoidal wave form plate fin heat sinks for laminar natural convection heat dissipation. *International journal of thermal sciences*, *208*, 109470. https://doi.org/10.1016/j.ijthermalsci.2024.109470

[11] Chiu, C. P., & Chou, H. M. (1993). Free convection in the boundary layer flow of a micropolar fluid along a vertical wavy surface. *Acta mechanica*, *101*(1), 161–174. https://doi.org/10.1007/BF01175604

[12] Ullah, Z., Abbas, A., Tariq, U., Haq, M. I. U., Kaynat, A., Bibi, A., Soha, T., Iqbal, M. W., & Ashraf, M. (2025). Gravity modulation analysis of heat transfer and magnetic boundary layer of MHD fluid along a vertical plate with variable viscosity and porous medium effects. *Computational environmental heat transfer*, *1*(2), 51–64. https://doi.org/10.62762/CEHT.2025.812351

[13] Ashfaq, M., Hajlaoui, K., Glili, I. El, Foukhari, Y., Arif, M., Shah, R. A., … & Khedher, N. B. (2025). Heat and mass transfer analysis of MHD boundary layer flow with motile microorganisms over porous surfaces under variable wall thermal conditions. *Thermal science and engineering progress*, *66*, 104056. https://doi.org/10.1016/j.tsep.2025.104056

[14] Yao, L. S. (1988). A note on Prandtl's tranposition theorem. *Journal of heat transfer*, 110(2), https://doi.org/10.1115/1.3250515

[15] Rubin, S. G., & Graves, R. A. (1975). Viscous flow solutions with a cubic spline approximation. *Computers & fluids*, *3*(1), 1–36. https://doi.org/10.1016/0045-7930(75)90006-7

[16] Kumari, M., Pop, I., & Takhar, H. S. (1997). Free-convection boundary-layer flow of a non-Newtonian fluid along a vertical wavy surface. *International journal of heat and fluid flow*, *18*(6), 625–631. https://doi.org/10.1016/S0142-727X(97)00024-6